HAL
open science

# Picosecond polarized supercontinuum generation controlled by intermodal four-wave mixing for fluorescence lifetime imaging microscopy

Pierre Blandin, Frédéric Druon, Marc Hanna, Sandrine Leveque-Fort, Christelle Lesvigne-Buy, Vincent Couderc, Philippe Leproux, Alessandro Tonello, Patrick Georges

## To cite this version:

Pierre Blandin, Frédéric Druon, Marc Hanna, Sandrine Leveque-Fort, Christelle Lesvigne-Buy, et al.. Picosecond polarized supercontinuum generation controlled by intermodal four-wave mixing for fluorescence lifetime imaging microscopy. Optics Express, 2008, 16, pp.18844-18849. hal-00567449

**HAL Id: hal-00567449**

**https://hal.science/hal-00567449**

Submitted on 30 Mar 2012

**HAL** is a multi-disciplinary open access archive for the deposit and dissemination of scientific research documents, whether they are published or not. The documents may come from teaching and research institutions in France or abroad, or from public or private research centers.

L'archive ouverte pluridisciplinaire **HAL**, est destinée au dépôt et à la diffusion de documents scientifiques de niveau recherche, publiés ou non, émanant des établissements d'enseignement et de recherche français ou étrangers, des laboratoires publics ou privés.

# Picosecond polarized supercontinuum generation controlled by intermodal four-wave mixing for fluorescence lifetime imaging microscopy

**Pierre Blandin,[1,2] Frederic Druon,[1,*] Marc Hanna,[1] Sandrine Lévêque-Fort,[2] Christelle Lesvigne,[3] Vincent Couderc,[3] Philippe Leproux,[3] Alessandro Tonello,[3] Patrick Georges[1]**

[1]*Laboratoire Charles Fabry de l'Institut d'Optique, CNRS, Univ Paris-Sud, RD 128 91127 Palaiseau, France*
[2]*Laboratoire de Photophysique Moléculaire, CNRS, Univ Paris-Sud, 91405 Orsay, France*
[3]*XLIM Institut de Recherche, CNRS, Univ Limoges, 123 avenue Thomas 87060 Limoges, France*
[*]*Corresponding author: frederic.druon@institutoptique.fr*

**Abstract:** We present the generation of a picosecond polarized supercontinuum in highly birefringent multimodal microstructured fiber. The initial steps of the spectral broadening are dominated by intermodal four-wave mixing controlled by the specific fiber design. Using a low repetition rate ultra-stable solid state laser, a pulse train well-suited for versatile time-domain fluorescence lifetime imaging applications is obtained.

©2008 Optical Society of America

**OCIS codes:** (060.4005) Microstructured fibers; (060.4370) Nonlinear optics, fibers; (060.2420) Fibers, polarization-maintaining; (320.6629) Supercontinuum generation General.

## References and links

1. P. Herman, H.J. Lin, J.R. Lakowicz, "Lifetime-Based Imaging," in *Biomedical Photonics Handbook* (CRC Press LLC, 2003)
2. R.W. Boyd, *Nonlinear Optics* (Academic Press, 2003)
3. K. Suhling, J. Siegel, P. Lanigan, S. Lévêque-Fort, S. Webb, D. Phillips, D. Davis, P.. French, "Time-resolved fluorescence anisotropy imaging applied to live cells," Opt. Lett. **29**, 584-586 (2004)
4. Z. Zhu T. Brown, "Experimental studies of polarization properties of supercontinua generated in a birefringent photonic crystal fibre," Opt. Express **12**, 791-796 (2004)
5. X. Xiong, W.J. Wadsworth, "Polarized supercontinuum in birefringent photonic crystal fibre pumped at 1064 nm and application to tuneable visible/UV generation," Opt. Express **16**, 2438-2445 (2008)
6. C. Lesvigne, V. Couderc, A. Tonello,P. Leproux, A. Barthélémy, S. Lacroix, F. Druon, P. Blandin, M. Hanna, P. Georges, "Visible supercontinuum generation controlled by intermodal four-wave mixing in microstructured fiber," Opt. Lett. **32**, 2173-2175 (2007)
7. N.G.R. Broderick, T.M. Monro, P.J. Bennett, D.J. Richardson, "Nonlinearity in holey optical fibers: measurement and future opportunities," Opt. Lett. **24**, 1395-1397 (1999)
8. J.M. Dudley, G. Genty, S. Coen, "Supercontinuum generation in photonic crystal fiber," Rev. Mod. Phys. **78**, 1135-1184 (2006)
9. J. M. Dudley, L. Provino, N. Grossard, H. Maillotte, R. S. Windeler, B. J. Eggleton, S. Coen, " Supercontinuum generation in air-silica microstructured fibers with nanosecond and femtosecond pulse pumping," J. Opt. Soc. Am. B **19**, 765-771 (2002)
10. T. Schreiber, J. Limpert, H. Zellmer, A. Tunnermann, K.P. Hansen, " High average power supercontinuum generation in photonic crystal fibers," Opt. Commun. **228**, 71-78 (2003)
11. S. Coen, A.H.L. Chau, R. Leonhardt, J.D. Harvey, J.C. Knight, W.J. Wadsworth, P.S.J. Russell, "Supercontinuum generation by stimulated Raman scattering and parametric four-wave mixing in photonic crystal fibers," J. Opt. Soc. Am. B **19**, 753-764 (2002)
12. M. Seefeldt, A. Heuer, R. Menzel, "Compact white-light source with an average output power of 2.4 W and 900 nm spectral bandwidth," Opt. Commun. **216**, 199-202 (2003)
13. A.B. Rulkov, M.Y. Vyatkin, S.V. Popov, J.R. Taylor, V.P. Gapontsev, "High brightness picosecond all-fiber generation in 525-1800nm range with picosecond Yb pumping," Opt. Express **13**, 377-381 (2005)
14. D.N. Papadopoulos, S. Forget, F. Druon, F. Balembois, P. Georges, "Passively mode-locked diode-pumped Nd:YVO4 oscillator operating at an ultralow repetition rate," Opt. Lett. **28**, 1838-1840 (2003)
15. S. Lévêque-Fort, D.N. Papadopoulos, S. Forget, F. Balembois, P. Georges, B. R. Masters, "Fluorescence lifetime imaging with a low-repetition-rate passively mode-locked diode-pumped Nd:YVO4 oscillator," Opt. Lett. **30**, 168-170 (2005)

#97073 - $15.00 USD Received 5 Jun 2008; revised 25 Jul 2008; accepted 29 Jul 2008; published 31 Oct 2008

16. C. Gerhard, F Druon, P. Georges, V. Couderc, P. Leproux, "Stable mode-locked operation of a low repetition rate diode-pumped Nd:GdVO4 laser by combining quadratic polarisation switching and a semiconductor saturable absorber mirror," Opt. Express **14**, 7093-7098 (2006)
17. V.E. Zakharov, S. Wabnitz, "Optical Solitons: Theoretical challenges and industrial perspectives," EDP Sciences, Springer, Berlin (1999)

## 1. Introduction

The past few years' progress in bio-photonics has enabled scientists to use fluorescence lifetime imaging as an in vivo and in vitro reliable tool for diagnostics [1]. The number of fluorophores used for such a technique has increased and their nature has diversified. All these probes (endogenous proteins, transfected fluorophores, quantum dots …) have various absorption bands and consequently cover a large excitation spectrum ranging from the ultraviolet to the infrared For the longest wavelengths, both the new generation of diode-pumped solid state lasers and the well-known Titane:Sapphire laser satisfy these requirements. For the blue and green part of the visible range, different strategies can be undertaken. The most current approach consists in generating secondary wavelengths in nonlinear materials, either in crystals (e.g. through harmonic generation), or in optical fibers with supercontinuum (SC) generation [2].

To measure multi-exponential decays, the fluorescence lifetime imaging microscopy (FLIM) in the time domain is preferred [1]. The principle is to excite the fluorophore with short pulses, and then to sample the fluorescence intensity decay. Such a technique requires sources which should necessarily satisfy several constraints in time domain. First, the pulse repetition period should be typically ten times longer than the fluorescence lifetime under study. To exploit the largest possible range of fluorophores, including fluorophores with long lifetimes, it is important to use an excitation source with a low repetition rate. Indeed, a repetition rate around few MHz gives access to lifetime up to tens nanoseconds. Second, the pulsewidth should be very short in comparison with the fluorescence lifetime, leading to values below 50 ps. Additionally, for such biological applications, optical beams with a high degree of polarization can be of considerable interest to explore the polarization dependence of images. This is the case for instance of fluorescence anisotropy measurement [3].

We propose here an alternative approach to generate broadband visible picosecond polarized laser light that would be ideal way to excite a wide range of fluorophores in FLIM experiments. This source is based on the generation of new spectral components obtained by intermodal four-wave mixing (FWM) in highly birefringent micro-structured optical fiber (MOF). The use of highly birefringent MOF may permit an extra degree of freedom for novel kind of SC spectral shapes keeping the output polarization state linearly polarized. [4, 5]. The MOF used here has already been studied in the nanosecond regime [6] to identify the mechanisms involved in spectral broadening. In the point of view of developing a system for FLIM applications, we carried out the study of this phenomenon in the picosecond regime. As expected we show that the SC generation results are slightly different than in the ns regime.

## 2. Microstructured fiber

Solid core MOFs surrounded by air holes have been widely used to generate supercontinuum light [7] because of their high nonlinearity and the possibility to engineer the dispersion by the control of the fiber geometry. The fabrication of polarization-maintaining MOFs has also been demonstrated by using an asymmetrical core. The processes involved in SC generation strongly depend on the MOF dispersion profile and effective core area. SC is also influenced by some input conditions like pulse duration or peak power. This is also the case of the laser carrier wavelength which in turn defines the normal or anomalous dispersion regime of propagation [8-10]. In our case, the spectrum of picosecond pulses is mainly broadened by FWM and Stimulated Raman Scattering (SRS) [11-13]. To extend the SC generation towards the visible part of the spectrum, we focused on a nonlinear effect that can be controlled through dispersion engineering: intermodal FWM [6]. By properly designing the air/silica

#97073 - $15.00 USD Received 5 Jun 2008; revised 25 Jul 2008; accepted 29 Jul 2008; published 31 Oct 2008
(C) 2008 OSA

structure of the core, one can modify the FWM phase-matching condition so to induce first a strong sideband in the visible domain, and then to stimulate further spectral broadening in the remaining part of the fiber effective length.

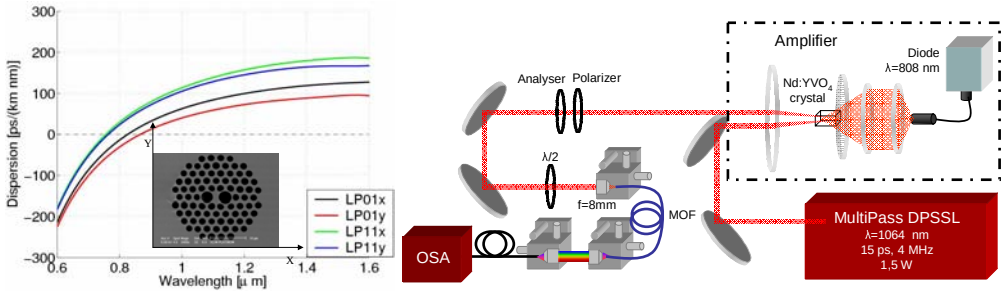


Fig. 1 (left). Numerically calculated dispersion of $LP_{01x}$, $LP_{01y}$, $LP_{11x}$, $LP_{11y}$ modes of the birefringent fiber and its profile (inset). (Right). Experimental setup. DPSSL means Diode-Pumped Solid State Laser.

A scanning electron microscope image of the air-silica MOF transverse structure is shown in fig. 1. The cladding is composed by a triangular structure of holes with an average diameter d=1.85 µm and a pitch Λ=2.6 µm, which yields a relative hole size d/Λ of 0.71. The solid core is sandwiched between two big holes with diameters of 3.3 µm and 3.6 µm. These holes break the π/3 symmetry inducing a strong phase and group birefringence. Using the commercial software COMSOL/FEMLab, we calculated the effective indices of the guided modes with a resolution of 25 nm. The values obtained enable us to estimate the phase and group birefringence (which respectively correspond to the effective indices difference and the group indices difference for the two polarizations state of the mode) for the fundamental mode at 1064 nm with a spatially transverse resolution of 55 nm: $B_\Phi = 2\times10^{-3}$ and $B_G = -3\times10^{-3}$. At this wavelength, the effective area of the fundamental mode is estimated to be 5.3 µm² and only four distinct linearly polarized core modes $LP_{01x}$, $LP_{01y}$, $LP_{11x}$, $LP_{11y}$ are guided. The corresponding numerically calculated dispersion parameters are also shown in fig.1. The zero-dispersion wavelength (ZDW) of $LP_{01}$ mode is around 827 nm (x polarization axis) and 866 nm (y polarization axis). The ZDWs of the $LP_{11x}$ and $LP_{11y}$ modes are located at 757 nm and 764 nm, respectively. Consequently, all the guided modes at the pump wavelength of 1064nm propagate in a largely anomalous dispersion regime.

## 3. Experimental setup

In order to meet the temporal requirements imposed by the FLIM applications, we used a home-made picosecond laser pump. This source was a 4 MHz rate mode-locked diode-pumped Nd:YVO4 laser followed by an amplifier which is also based on a Nd:YVO4 crystal (fig 1). The ultra low-repetition rate oscillator consisted of a long multi-pass cavity, developed to perform fluorescence lifetime imaging of fluorophores with long fluorescence lifetime [14, 15]. We used a dual mode-locking technique to increase the laser stability [16]. The laser delivered an average power of 1.5 W at 4 MHz with pulse duration of 15 ps and pulse energy of 0.38 µJ. The amplifier consisted of a dual pass amplifier using a 10-mm long, 0.1%-doped Nd:YVO4 crystal pumped with a 400-µm-diameter-fiber-coupled diode delivering up to 30 W. At the amplifier output, the power of the IR beam was 4.5 W, corresponding to 75 kW peak power with a good spatial quality (M² factor of 1.3). We adjusted the power focused on the fiber with a polarizer and an analyzer placed in the infrared beam pathway. A half-wave plate was used to control the input polarization state, and the injection of this IR beam in the MOF was realized thanks to 8 mm aspherical lens objective and a three axis flexure stage. The spectrum was measured using an optical spectrum analyzer (OSA) on the 350-1750 nm range with a precision down to 1 nm.

#97073 - $15.00 USD Received 5 Jun 2008; revised 25 Jul 2008; accepted 29 Jul 2008; published 31 Oct 2008
(C) 2008 OSA

## 4. Results

We performed the first series of experiments with a 1.4-m-long of MOF. This choice of length allowed us to identify the FWM peaks before they are completely blurred by subsequent spectral broadening, while still demonstrating the possibility to obtain large excitation spectra around the FWM peaks. To clearly identify the nonlinear phenomena responsible for this broadening, we studied first the spectra generated in the MOF under different polarizations and input powers. Since this fiber is polarization-maintaining, the resulting SC is mainly co-polarized with the input beam. During the experiments, we have observed spatial excitation-dependent phenomena. However, the reported results only concern the case where both spatial $LP_{01}$ and $LP_{11}$ modes were excited. Moreover, all the results hereafter presented have been obtained with a coupling efficiency varying from 8% to 10%. Under the best coupling conditions a maximum of 2.15 kW peak power can be injected into the fiber. As shown in fig. 2, the IR part of the SC seems not particularly influenced by the input polarization state of the pump. Starting from a coupled average power of 50 mW or beyond, a flat and smooth continuum from 1 µm to over 1.75 µm is generated. Since this generation is polarization-independent, this result can be interpreted in terms of modulation instability, higher order soliton fission and Raman scattering in anomalous dispersion. These phenomena follow the nearly isotropic nature of the fiber nonlinearity and they do not require any phase matching to be satisfied.

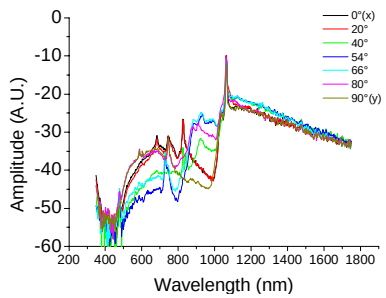


Fig. 2. Spectra generated in the MOF of 1.4 m versus polarization and for an output power of 120 mW.

Differently, the fraction of the SC which falls in the visible domain exhibits clear polarization dependence (fig. 2). One can notice that the number of peaks and peak wavelengths strongly differs from a polarization to another. Moreover, the visible SC obtained in the ps regime clearly indicated more peaks and a less smooth shape than the SC obtained in the ns regime [6]. In order to analyse the SC generation process and to observe the order of appearance of the different spectral components, we plotted the SC along x and y versus input power. With a polarization state parallel to the fiber y axis (fig. 3, left), a first peak at 746 nm appears from 90 mW of coupled average power. In the best conditions, the average power for a 20 nm range centred at 746 nm was measured around 0.9 mW. This sideband has already been observed in the same type of MOF using a nanosecond laser of the same central wavelength [6]. This sideband appears when the laser pump is carried by an equal combination of $LP_{01y}$ and $LP_{11y}$ modes. Such modal FWM would also imply a corresponding Stokes sideband at 1854 nm which is out of the detection range of our optical spectrum analyzer (OSA). We also experimentally verified that such sideband is carried by a mode of type $LP_{11}$ as predicted by the phase matching condition (see also Ref.6 and references therein). In our experiment the pump power is large enough to permit us to study the bimodal FWM in the strong conversion regime. At higher power, this peak enlarges and other spectral components become detectable. Moreover, other secondary peaks appear corresponding to more complex interactions like combination of modal, vector FWM and cross phase modulation. This multiple peaks appearance is even more clear in fig. 3 in the case of an input pump linearly polarized along the fiber x axis. An important peak at 826 nm and a smaller at 746 nm appear starting from 60 mW of coupled average power. The higher peak corresponds to the anti-Stokes wave of

#97073 - $15.00 USD Received 5 Jun 2008; revised 25 Jul 2008; accepted 29 Jul 2008; published 31 Oct 2008
(C) 2008 OSA

bimodal FWM on the x-axis, and exhibits in the best conditions an average power around 1.2 mW for a 20 nm range centred at 826 nm. In this case we can also distinguish the corresponding Stokes wave at 1495nm. As shown in fig. 2 the peak at 746 nm is equivalently present both on x and y polarizations. Whereas a clear phase matching has been identified for the y-axe and since no depolarization has been observed on the visible SC, it seems that this peak would also correspond to a bimodal FWM. We also verified experimentally that SC fraction falling in the visible domain is carried by a $LP_{11}$ mode while the IR fraction is carried by a $LP_{01}$. Regardless of the polarization, one can notice strong shape differences compared to ns regime. In fact, the ps SC is more spiky and extends much less toward the blue.

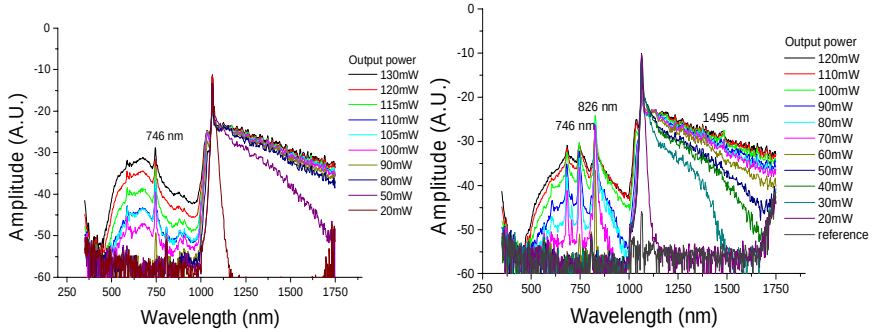


Fig. 3. Spectra generated in the MOF of 1.4 m versus coupled average power for polarization along the y axis (left) and the x axis (right).

## 5. Discussion

Numerical simulations were performed to study supercontinuum generation from modal FWM with picosecond pump pulses, in order to understand the differences with the ns regime. The main physical difference is that the walk-off length of ps pulses can be shorter than the physical length of the MOF. In this case, phase matching and temporal overlap of the pump modes should be both satisfied to have an efficient FWM. This is the reason why moving from nanosecond laser to picosecond lasers one can obtain qualitatively different results even using nearly the same peak power. To exemplify the two situations we have numerically simulated the supercontinuum generation for a pump divided in modes and polarization state in a MOF of 1.8 m. Our numerical results are shown in fig. 4. We assumed an input peak power per mode and per polarization state of 550 W, which means 2200W of total peak power. With a repetition rate of 4MHz, this is nearly 130mW, so in principle the simulated power has the same order of magnitude of what is measured in the experiments. The fiber length has been chosen to clearly identify and understand the mechanisms involved. We show the corresponding output spectrograms [8] for pulse duration of 15 ps (left inset) and 40 ps (right inset). We numerically solved the four coupled nonlinear Schrödinger equations (two modes and two polarizations) with the MOF parameters in use. Our governing equations can be found in Ref.17, pp.250-252. Differently from Ref.17 we also included the Raman response for each equation. With a spectrogram we can supply a further insight on the different results obtained for picosecond or nanosecond pulses. For short pulses (15 ps) the walk-off of the two pump modes has a large impact on nonlinear visible continuum build-up by stopping the FWM conversion efficiency. Moreover no cross phase modulation is possible between the 800-900 nm range and the wavelengths longer than 1064 nm, since there is no time overlap for these wave-packets. Note that the anti-Stokes wave-packets in the ps-regime are tightly confined in both the frequency and time domains (Fig. 4 (left) for the $LP_{11x}$ and $LP_{11y}$ modes, around 800 nm and around 20-25 ps). On the right inset of fig. 4 we show the same spectrogram with 40 ps pulses. In this case the FWM conversion efficiency is high as well as the time overlap between pump, Stokes and anti-Stokes wave-packets. This fact also explains why the FWM is far more efficient with nanosecond laser than with the present picosecond source. The anti-Stokes pulses may also excite further spontaneous Raman

#97073 - $15.00 USD Received 5 Jun 2008; revised 25 Jul 2008; accepted 29 Jul 2008; published 31 Oct 2008
(C) 2008 OSA

scattering. Note also the time overlap between the visible and the IR spectrum with the possible effect of cross-phase modulation, which is responsible for spectrum flattening observed at longer pulses. However in this case, the visible spectrum is less localized in time, and may eventually have an envelope longer than the typical fluorophore lifetime to be imaged. Besides modal FWM one can observe the vector FWM which takes place with a pump divided in polarization state and carried by a unique guided mode. Given the fact that the polarization birefringence is lower than the modal birefringence, these sidebands are much closer to the pump. This fact explains the peaks at 980 nm observed in the simulated spectrum. These experimental and numerical investigations confirm, such as in [4, 5], that, with this kind of fibers exhibiting particular asymmetrical geometry, the spectra and the polarization are strongly correlated and reveal that the transition in spectral shaping occurs in the ten picosecond regime. Nevertheless, the spectral broadening observed in picosecond regime is seeded by sharp lines generated by modal FWM. Their related spectral positions are determined by the phase matching of FWM which in turn is mainly influenced by the fiber structure and by the laser wavelength. By designing properly the fiber, one can therefore generate specific wavelengths in the absorption band of the fluorophores and seed the SC around these wavelengths. Further broadening around these seeded wavelengths can then lead to a wide spectrum in the band of investigation.

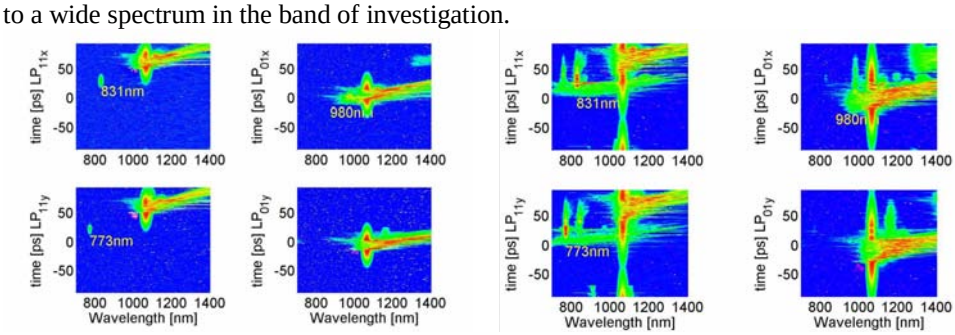


Fig. 4. Numerically calculated spectrograms at the output of 1.8 m of MOF. The peak power is of 550 W per mode and per polarization state. (Left): with pump pulses of 15 ps. (Right). With pump pulses of 40 ps

## 6. Conclusion

In conclusion, we have developed a broadband polarized laser source in visible domain dedicated to FLIM. The spectral broadening is controlled by intermodal FWM in highly birefringent multimodal MOF. The obtained visible continuum profile is drastically affected by the temporal walk-off between transverse modes involved in non linear conversions. Using an ultra stable low repetition rate picosecond mode-locked oscillator, we are able to satisfy the temporal constraints inherent to the time domain FLIM. The present MOF permit us to generate spectral bands at 826 or 746 nm or a combination of them according to the choice of the polarization state of the laser input. We demonstrated that the SC generation in picosecond regime in highly birefringent MOF strongly differs compared to standard MOF. By modifying the fiber structure one can engineer the FWM to generate intense visible radiation mainly localized in spectral regions of interest for FLIM imaging. We believe that the full understanding of vectorial and intermodal FWM phase matching aspects in SC generation will lead to the development of versatile laser sources for a wide variety of biological imaging applications.

## Acknowledgments

This research was partially supported by the research program Pôle Laser (2000–2006) and the MRCT (Mission Ressources et Compétences Technologiques) from the CNRS.

#97073 - $15.00 USD Received 5 Jun 2008; revised 25 Jul 2008; accepted 29 Jul 2008; published 31 Oct 2008
(C) 2008 OSA